*16th World Conference on Earthquake, 16WCEE 2017*

*Santiago Chile, January 9th to 13th 2017*

*Paper N° 2518*

*Registration Code: S-I1452367670*

# AN ECONOMIC SLIDING ISOLATION SYSTEM FOR LIGHT FRAME RESIDENTIAL STRUCTURES

E. Jampole(1), G. Deierlein(2), E. Miranda(3), B. Fell(4), S. Swensen(5), C. Acevedo(6)

*(1) Graduate Student, Stanford University, ezra.jampole@gmail.com*
*(2) Professor, Stanford University, ggd@stanford.edu*
*(3) Associate Professor, Stanford University, emiranda@stanford.edu*
*(4) Associate Professor, California State University, Sacramento, fellb@ecs.csus.edu*
*(5) Associate, Exponent, sswensen@exponent.com*
*(6) Graduate Student, Stanford University, cacevedo@stanford.edu*

## *Abstract*

Experience from past earthquakes has shown that light frame residential houses in the United States typically pose a low collapse risk, but they are susceptible to damage that can lead to significant financial loss and displacement of residents. The authors have developed a low-cost seismic isolation system that uses standard construction details and balances isolator displacement demands with base shear force demands through a high-friction sliding system. The isolation system consists of high-density polyethylene sliders on a flat or concave galvanized steel sliding surface, with a sliding coefficient of friction between 0.15 and 0.25 at the isolation interface. The inherent strength and low mass of light frame residential construction allows for a high-friction isolation system to effectively eliminate superstructure damage during even large earthquakes. Parametric studies have shown that high friction interfaces economically reduce isolation displacement demands. Isolator sliding material and component tests have been conducted to characterize velocity and pressure dependent interface friction properties of the sliding isolators. Shaking table tests of a full-scale light framed isolated house have been conducted at the shared-use NEES facility at the University of California at San Diego. Results of these tests presented herein have (a) confirmed that the isolation system can effectively eliminate damage to the light frame superstructure under repeated severe earthquake ground shaking (b) validated nonlinear computer models to determine sliding isolator and superstructure performance, and (c) demonstrated the constructability and economic practicality of the proposed details for the foundation and wood-framed first floor isolation platform.

*Keywords: Sliding seismic isolation; High-friction isolation; Light frame housing; Full-scale shake table test.*

## 1. Introduction

It is widely recognized that seismic isolation is one of the most effective-methods to prevent or eliminate damage to buildings during large earthquakes. Isolation has not been extensively used in the United States because of numerous design impediments [1]. Light frame structures in particular could benefit from the use of seismic isolation because of the ease with which they are damaged during earthquakes, with cosmetic damage occurring in sheathing and stucco at drifts as low as 0.17% [2]. While light frame structures generally do not collapse, there can be enormous insured losses and large numbers of displaced residences, such as following the 1994 Northridge, California earthquake [3] [4].

Seismic isolation has been successfully implemented in thousands of buildings and light frame structures in Japan [1] [5], and investigators have confirmed exceptional performances of elastomeric, rolling, and sliding isolated light frame houses [6] [7] [8]. Numerous researchers have found that elastomeric isolators are difficult to implement for light frame structures because they are too stiff for light structures [7] [9] [10] [11]. On the other hand, friction pendulum isolation systems can reduce story drifts to one third of fixed-base demands [8]. Unfortunately, researchers have noted that much of the cost of isolating light frame structures comes from the cost of commercial isolators and construction costs related to using very rigid steel isolation plane diaphragms [8] [12].

The authors have proposed a sliding isolation made of off-the-shelf parts that limits isolation displacements by using a high-friction sliding interface on either a flat or concave sliding surface [13]. Due to the low mass of light frame structures, light frame structures lend themselves to sliding isolators, and do not experience damaging levels of drift even with isolation interface coefficients of friction between 0.15 and 0.25. The high friction interface limits median isolator displacements in high-seismic regions to about 25 cm [13]. The high friction isolation system is tested in conjunction with a "unibody" superstructure as part of a larger Network for Earthquake Engineering Simulation (NEES) project. The unibody superstructure integrates structural and nonstructural wall systems through adhesives and enhanced fasteners to engage finishes, resulting in walls that are two times stronger and stiffer than conventional light frame walls [14] [15]. Full-scale shake table tests of the prototype high-friction isolated house presented here verify design and construction procedures of isolators and a timber framing isolation plane, while validating numerical models of isolation behavior and the dynamic response of light frame structures on top of high friction sliding isolation. A full summary of testing can be found in Jampole et al. (2016) [16]. Details regarding testing the fixed-base house can be found in Acevedo et al. (2017) [17].

## 2. Test Structure Description

A full-scale two story wood frame isolated house was constructed. The house is representative of single-family homes in California. The plan dimensions were 7.07m x 11.34m. The total floor area was around 160 m$^2$ and the weight, W, was around 305 kN.

The isolation plane was constructed of conventional wood framing, as is shown in Fig. 1. LVL beams cantilever over isolation bearings to support the exterior walls. The length of the cantilever was determined by the magnitude of anticipated isolation displacements, such that the perimeter of the house covers the foundation. This eliminates the need for an isolation moat. Plywood sheathing was attached to the top of LVLs and wood joists with adhesives and screws to increase rigidity of the first floor diaphragm. The ability to construct a first floor diaphragm with conventional wood framing represents a significant cost saving as additional subcontractors were not required for construction of the first floor diaphragm, as is often required for steel or concrete first floor diaphragms of isolated light frame structures.

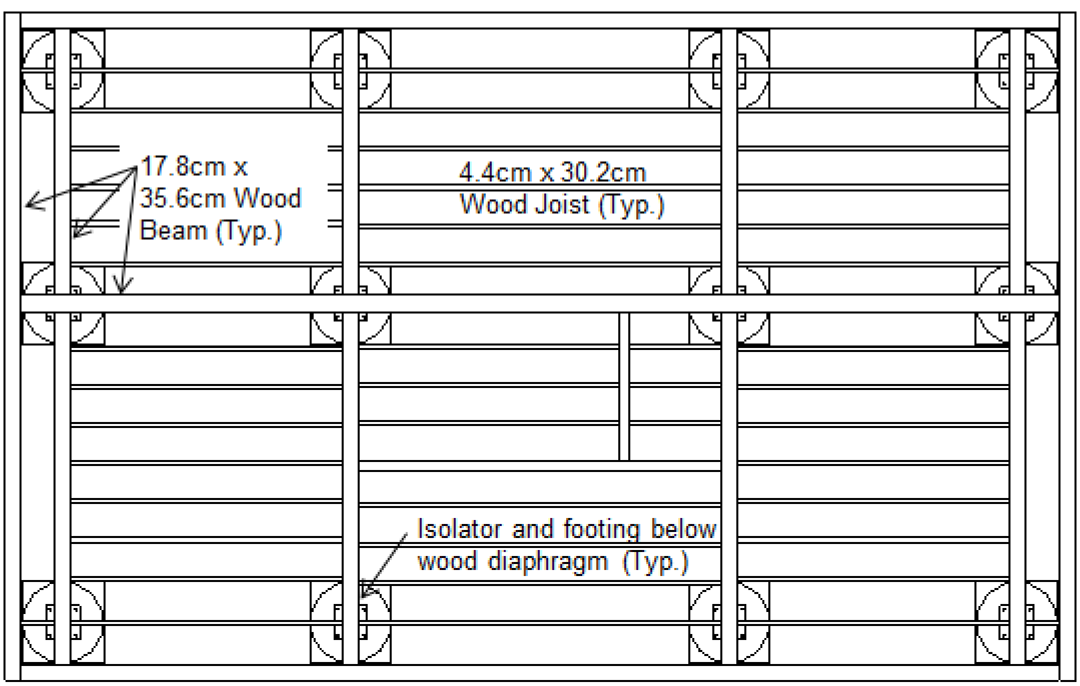


Fig. 1 – First floor wood-framed diaphragm.

The sliding isolators were attached to the bottom of the first floor diaphragm at twelve locations, as shown in Fig. 1, and per cross section in Fig. 2. Isolators were high-density polyethylene (HDPE) disks 94mm in diameter and 13 mm thick. They are placed in a recess in stainless steel backing plates, connected to a swivel bearing on the underside of the LVLs that allows for rotation of the bearing unit. The isolators slide on a galvanized steel plate attached to the top of a grout footing. In the first sequence of tests, the plate was concave with a radius of curvature, R = 2m, providing a restoring stiffness of K = W/R = 153 kN/m. These tests are referred to as dish tests and a sample dish isolator during testing is shown in Fig. 3. Following dish tests, the concave sliding surface was replaced by a flat sliding surface with no added restoring component. HDPE sliders were also replaced between the test phases. Fixed-base testing was conducted following the completion of isolation testing.

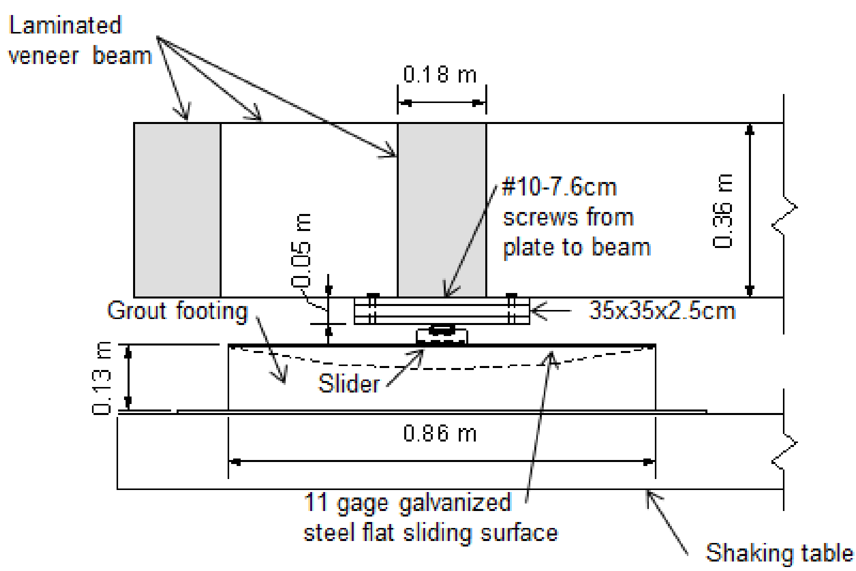


Fig. 2 – Cross-section of the flat sliding isolation system.

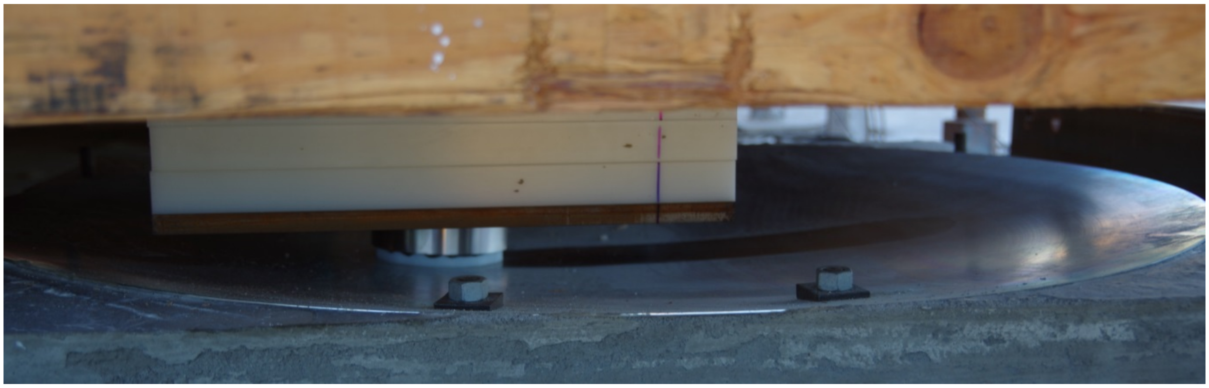

Fig. 3 - Sliding on concave "dish" surface.

The average pressure on the HDPE sliders was 3.8 MPa, which is significatly less than pressures at isolation interfaces in conventionl larger building applications. Thermoplasitcs sliding on galvanized steel have velocity and pressure-dependent coefficients of friction, with higher pressure corresponding to lower friction. With the low pressure interface, it was expected that the coefficient of friction would be between 0.17 and 0.22, based on friction characterization tests conducted at pressures similar to those scene in th house at sliding velocities of 0.3 to 0.4 m/s, and accounting for variability.

## 3. Shake Table Testing Procedures

The full-scale house shown in Fig. 4 was tested on the outdoor shake table at the NEES at University of California, San Diego (UCSD) facility. Tire impact tests at the roof and white noise excitation were used to determine the period of the house prior to activation of the isolation system. The measured first and second mode periods were 0.14 and 0.06s with 2% damping.

Fig. 4 - Full-scale sliding isolated house at NEES@UCSD.

The house was subjected to seven ground motions in both the flat and dish isolation configurations. Ground motions were selected to validate analysis models of isolation systems. The peak ground acceleration ranged from 0.55g to 1.59g, and the peak ground velocity ranged from 97 cm/s to 160 cm/s. The response spectrum of the selected records represent records that could be used to match the MCE spectrum for an isolated house with coefficient of friction, $\mu = 0.18$ in a high seismic zone in California. Additional details regarding ground motion selection can be found in Jampole et al. (2016) [16].

## 4. Experimental Results

While the house was subjected to seven ground motions in each isolation configuration, results presented here will focus on the response to the Capitola 000 recording from the 1989 Loma Prieta earthquake, which was scaled by a factor of three. This ground motion was used with various scale factors in the fixed-base phase of testing as well.

Of primary concern in the design of seismic isolation systems is the peak sliding isolation displacement, thus much attention is placed on this demand parameter. Fig. 5 shows the ground acceleration and relative isolation displacement history of the flat and dish system subjected to Capitola 000 (x3). Horizontal lines are drawn on the ground acceleration history plot at +/- 0.18, indicating the coefficient of friction of the system at high sliding velocities. Since friction is velocity-dependent, sliding will initiate at lower velocities, however, significant sliding excursions can occur when the ground acceleration exceeds the coefficient of friction. For Capitola 000 (x3), this occurs at many instances, leading to many sliding excursions and changes in sliding direction. The largest sliding excursions occur when there is a combination of high acceleration and long pulse duration, such as the pulses initiating at 8 s, 8.7 s, and 9.2 s. The most noticeable effect of the dish isolators is the restoring capability. When sliding is around zero relative displacement, the restoring force is low, thus the sliding displacement history is roughly the same for the flat and dish systems. This is seen in the sliding response history up to 8 s. When larger pulses cause sliding far up the dish (away from zero relative displacement) the restoring component is larger and somewhat limits the peak isolation displacement, as can be seen at the sliding excursion beginning at 8 s. Once at the top of the dish, the force of gravity from being on a concave surface restores the system to near zero displacement.

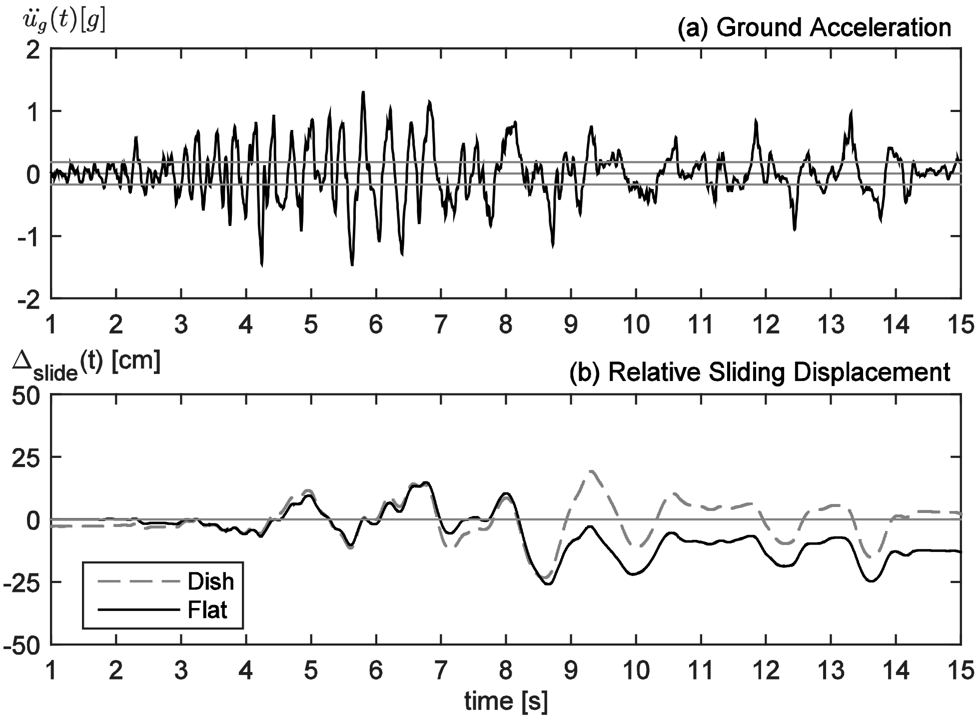


Fig. 5 – Flat and dish isolator response history of house subjected to Capitola 000 (x3). (a) ground acceleration; and (b) relative sliding displacement.

A completely rigid superstructure would have uniform acceleration in the superstructure during shaking equal to the ground acceleration when not sliding and to the coefficient of friction during sliding. While the unibody house has a short period of 0.1s when fixed and 0.14s when isolated prior to sliding, the structure is not sufficiently rigid to have near uniform acceleration in the superstructure. Fig. 6 shows the relative sliding displacement history and absolute floor acceleration history when the flat isolated house is subjected to Capitola. At the initiation of each sliding excursion, acceleration fluctuations occur due to the stick-slip at the isolation interface. As the structure begins to slip relative to the ground, it first slips at the ground while the structure continues moving. High frequency vibration occurs, centered around the second floor, which experiences acceleration close to the "rigid-body" acceleration equal to the coefficient of friction of 0.18. The sliding of the structure represents a first rigid body mode, while the acceleration fluctuations represent a second vibration mode of a free-free structure.

The relative sliding displacement and floor acceleration histories of the dish system subjected to Capitola are shown in Fig. 7. Just as in the response to the flat system, a higher mode is excited in the superstructure at the beginning of sliding excursions. The offset value about which the roof and first floor accelerations vibrate increases as the structure slides up the dish. The peak accelerations expected for a rigid body would occur at the end of a slide at the top of the dish, while the peak acceleration fluctuation occurs at the beginning of sliding excursions going up the dish. For sliding excursions that initiate at the top of the dish going down the dish, such as at 5s, the friction and restoring component of the offset acceleration value counteract each other, until the structure begins sliding up the other side of the dish. Friction forces, high restoring from being far from the bottom of the dish and sliding up the dish, and the peak acceleration fluctuation therefore do not generally occur at the same time, preventing higher accelerations. The acceleration fluctuations are damped out by the end of most sliding excursions up the dish to prevent them from acting in concert with the restoring component. One need only worry about a situation in which sliding begins in the direction heading up the dish from a position already far up the dish.

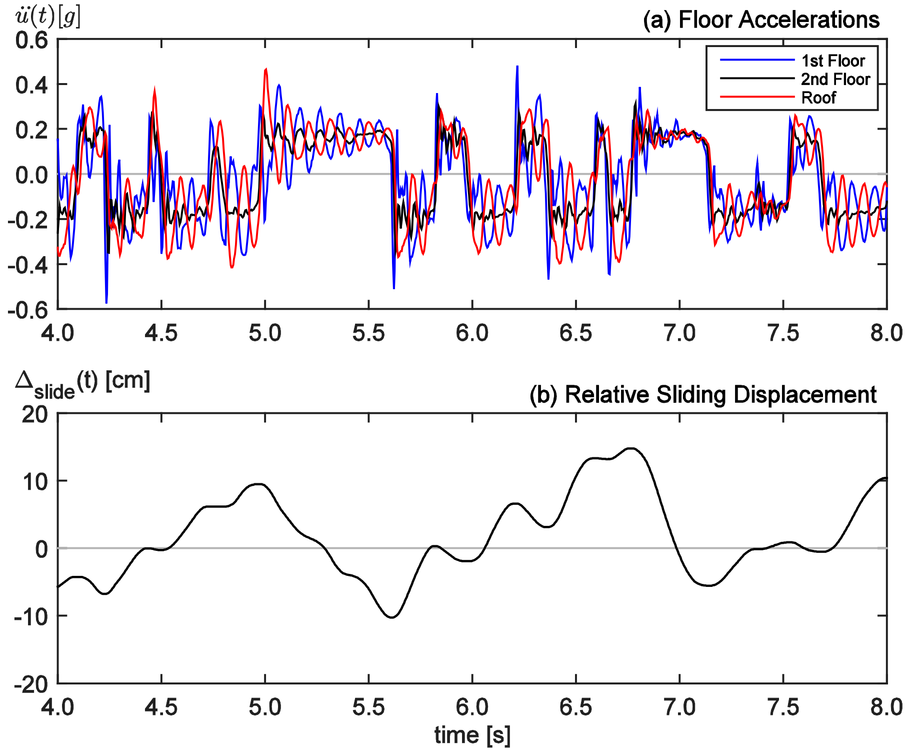


Fig. 6 – Response of flat sliding isolated house to Capitola (x3). (a) floor accelerations; and (b) relative sliding displacement.

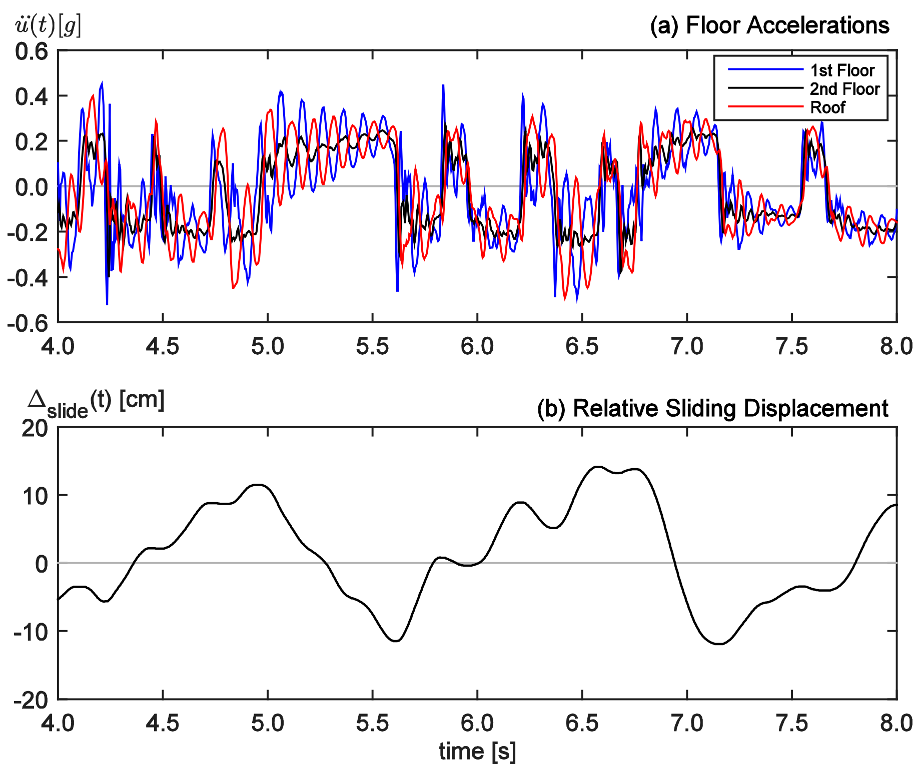


Fig. 7 – Response of dish sliding isolated house to Capitola (x3). (a) floor accelerations; and (b) relative sliding displacement.

The peak floor acceleration of the house in response to Capitola was 0.58g during the flat test and 0.52g during the dish test. Both of these occurred at 4.2s. It is somewhat surprising that the flat system has higher acceleration, but is explained by the fact that the fluctuation begins at the initiation of sliding down the dish at a relative displacement of 5cm up the dish, thus the friction force and restoring force counteract each other for the dish system.

Despite the high peak floor accelerations, this does not necessarily translate into higher forces at every level, as the forces at a particular level is the summation of the mass times the acceleration above that levels. For example, the sum of the forces acting at the isolation interface level, which controls the design of the connection of sliders to the superstructure, is calculated in Eq. 1

$$\Sigma F_{ISO} = M_1\ddot{u}_1(t) + M_2\ddot{u}_2(t) + M_3\ddot{u}_3(t) \tag{1}$$

Lumping wall weights to each level, the distribution of weights to each floor are approximately: 1st floor = 75 kN, 2nd floor = 110 kN, and roof = 120 kN. Normalized isolator hysteresis of the flat and dish systems subjected to Capitola are shown in Fig. 8. Dashed lines are drawn to shown the theoretical forces that would act on a rigid body. Because the first floor and roof acceleration are out of phase, their effect on forces at the isolation level is mostly mitigated. The flat system is seen to have almost box like hysteresis, with only small variation from the rigid body approximation. Similarly, the dish has trapezoid-like hysteresis at the isolation level. Variations from the rigid-body response can be attributed to the fact that the mass of walls, a significant portion of the weight of the structure, is actually distributed up the height of the structure and has different acceleration at each location, rather than the assumption of being lumped at each level. Additionally, stick slip at the isolation interface likely causes some of the spikes in isolation system forces.

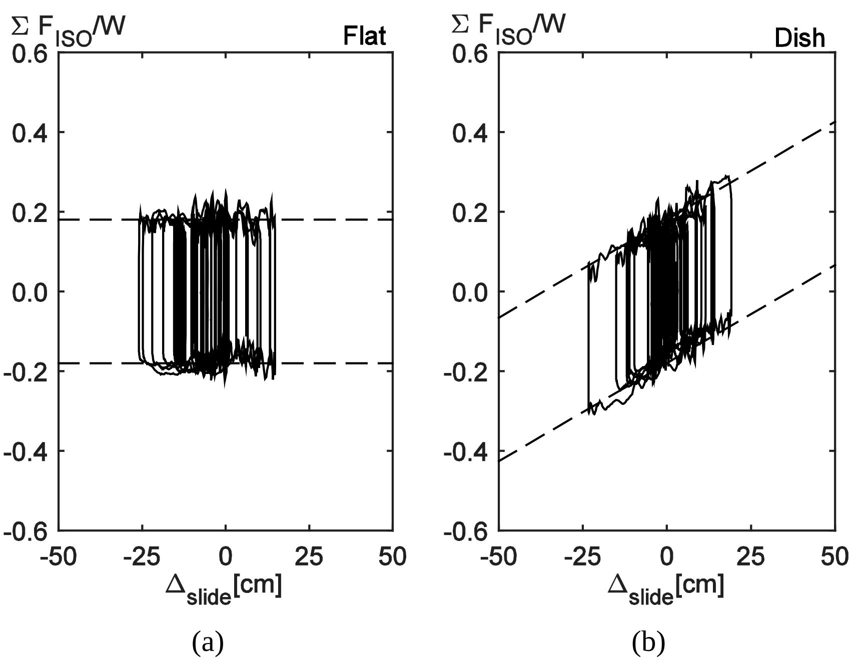


(a) (b)

Fig. 8 – Isolator hysteresis when subjected to Capitola (x3). (a) flat; and (b) dish.

Story shear ratio, SSR, is computed as the lateral force at the first story normalized by the superstructure weight, $W_{ss}$, and the peak SSR throughout the response history is the seismic coefficient for the superstructure above the isolation system. SSR is calculated as in Eq. 2:

$$SSR = \left(M_2\ddot{u}_2(t) + M_3\ddot{u}_3(t)\right)/W_{ss} \tag{2}$$

In the calculation of SSR, the first floor mass and acceleration are not included as they were in calculating forces at the isolation level. The out of phase accelerations at the first floor and roof therefore do not somewhat mitigate each other. Large fluctuations in SSR are seen at the beginning of sliding excursions. SSR versus sliding displacement "hysteresis" are shown for the flat and dish house subjected to Capitola in Fig. 9. For this ground motion, the peak SSR is 0.36 for both systems. For the flat system in particular, this indicates an amplification of a factor of two over the rigid body expected value of the coefficient of friction = 0.18.

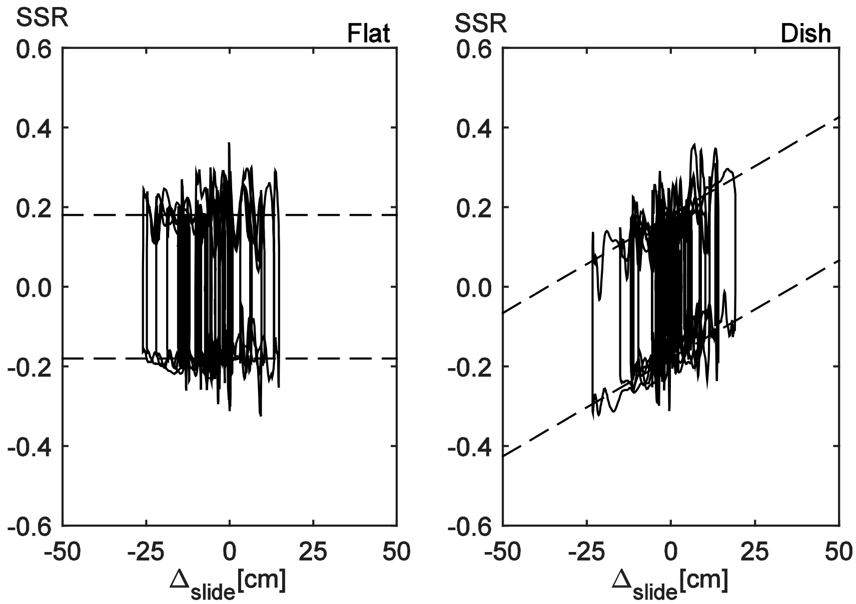


(a) (b)

Fig. 9 – SSR versus sliding displacement of house when subjected to Capitola (x3). (a) flat; and (b) dish.

Despite what might be considered large values of SSR, measured drifts in the superstructure were very small. Fig. 10 shows the first story wall hysteresis (SSR versus Drift). The peak drift is less than 0.2cm, with story drift ratios of 0.07% and 0.08% in the flat and dish isolated houses, respectively. Drift data is noisy, largely because of the difficulty in measuring drifts that are very tiny. The second story of the house experienced virtually zero story drift.

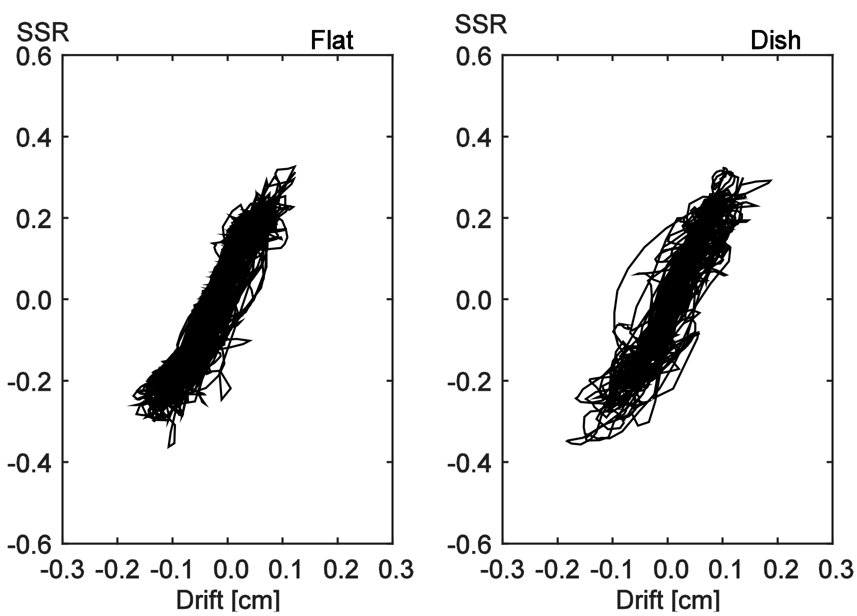


(a) (b)

Fig. 10 – First story wall hysteresis of isolated house when subjected to Capitola (x3). (a) flat; and (b) dish.

Barely any damage was observed during testing, save for a few popped screws in small corner cracks. This damage is typical of construction and may have been caused by locally jacking the house to replace isolators in between the dish and flat isolator testing phases.

## 5. Numerical Modeling

Numerical models that capture the behavior of the house during shaking can be used for determining the effects of numerous untested items. For example, the high friction isolation system could be implemented with more levels, different aspect ratios, coefficients of friction, mass distribution, with different story strength and stiffnesses from conventional walls, and with the inclusion of the vertical component of the ground motion. It is important to quantify the amplification of story shear ratios from the high frequency dynamics observed during testing. Fig. 11 shows a schematic diagram of a frame model of half the house, made in OpenSees [18]. Mass is lumped at each level, which is assumed to be rigid. Diagonal elements link levels to transfer lateral loads, and rigid vertical elements transfer vertical loads. Diagonal elements stiffness is calibrated such that when the house is fixed at the first floor, the period of the house is the same that measured during fixed base testing. A pressure and velocity-dependent friction model for HDPE on galvanized steel determined from material characterization tests is used at the sliding interface at the base of the structure. Vertical flexibility of the isolators is included to account for the flexibility of the cantilevered walls at the first floor.

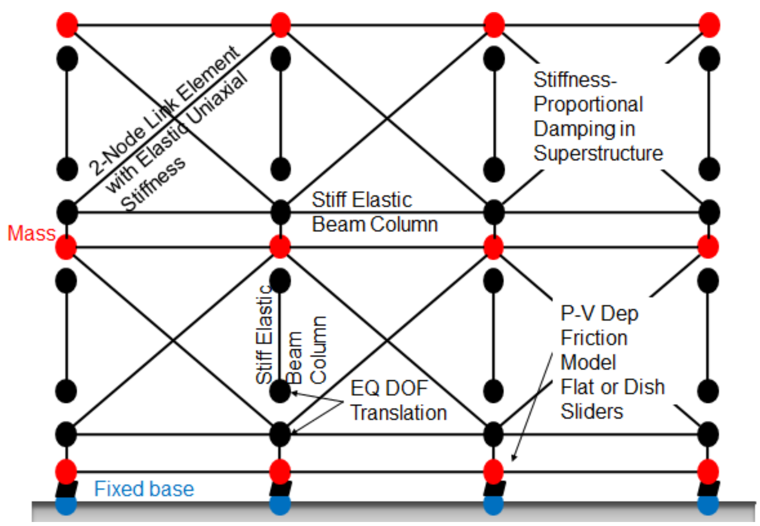


Fig. 11 – Schematic diagram of frame model of isolated house.

The most important parameters to accurately mimic house behavior are the sliding displacement history and the story shear ratio, as these are the controlling design parameters for the response of the isolation system and for the forces in the superstructure, respectively. Fig. 12 compares measured and predicted sliding displacement when the dish system was subjected to Capitola. The model captures the entire response history very well. Note that the tested house began with a small residual displacement from the previous ground motion that was not included in the model.

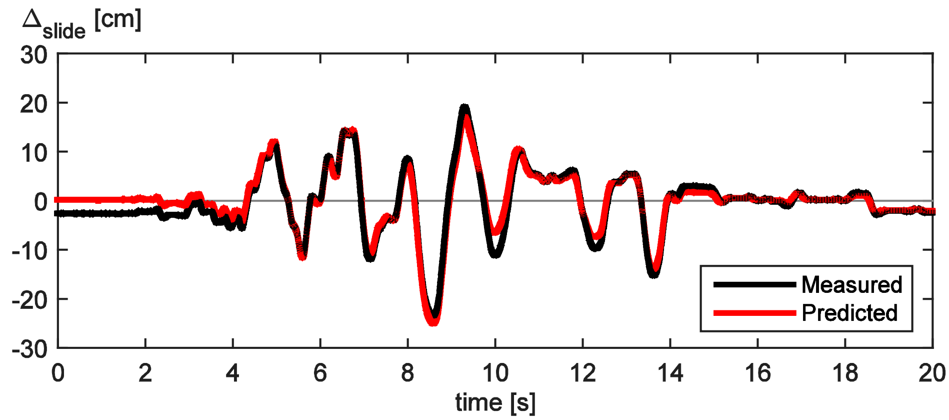


Fig. 12 – Measured vs. predicted sliding displacement history of dish isolated house subjected to Capitola (x3).

The measured and predicted SSR histories for a portion of the response history are shown in Fig. 13. The model captures the fluctuations in first story forces due to the superstructure vibration mode during sliding. Importantly, the peak SSR is captured by the frame model.

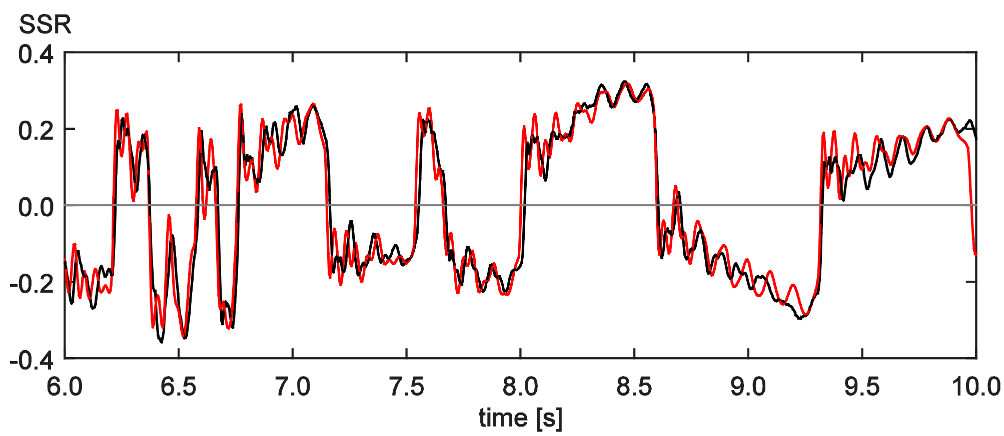


Fig. 13 – Measured versus predicted story shear ratio of dish isolated house subjected to Capitola (x3).

## 6. Conclusions

Seismic isolation has repeatedly been shown to significantly improve the performance of structures during large earthquakes by concentrating deformation at the isolation level. The authors have conducted full-scale shake table tests to demonstrate a cost-effective sliding isolation system for light frame residential structures. Using high friction sliding isolators made of HPDE reduces peak isolation displacements, which enables a conventional wood framing plan for the first floor with cantilever overhangs that cover the extent of the galvanized steel sliding surface and spread footing. The presence of a restoring force through sliding on a concave dish reduces both peak isolation displacement and ensures small residual isolation displacements. The isolation system was shown to be durable as each set of isolators and sliding surfaces experienced seven strong ground motions.

Inertial forces from the superstructure were seen to be amplified by a factor of two over expected values for a completely rigid system. The second mode of the sliding structure is activated at the initiation of sliding (the first mode), and is the source of the high frequency dynamic response during sliding. Peak story shear ratios (~0.38) were roughly the same in the flat and dish system because the friction force and restoring force in the dish system act counter to each other when the dynamic response in the superstructure is at its highest. Despite the larger than expected story shear forces, demands are low for light frame house, especially one using a unibody superstructure with enhanced strength and stiffness. The peak story drift ratio observed during all ground motions was only 0.09% drift, well below the threshold for damage.

A frame model created using OpenSees is shown to well-predict the sliding displacement history and first story SSR. The model lumps mass two points above the isolation supports at each level and using diagonal struts to transfer lateral loads. It can be used in future studies to assess the influence of different isolation or superstructure properties, or to include the vertical component of the ground motion in analyses. This will be useful for making design recommendations for isolated light frame structures.

## 7. Acknowledgments

This material is based upon work supported by the National Science Foundation (NSF) under CMMI-NEES Grant No. 1135029. Additional financial support was provided by NSF through student fellowships, an EERI Graduate Student Fellowship, and the Blume Earthquake Engineering Center at Stanford University. Donation of materials and supplies is greatly appreciated from Simpson Strong-Tie, PPG Industries, Alabama Metal Industries Corporation (AMICO), and Albion Engineering. Any opinions, findings, and conclusions or recommendations expressed in this material are those of the authors and do not necessarily reflect the views of the National Science Foundation or other sponsors.

The authors would also acknowledge the technical input and advice of a talented group of professional consultants including: K. Cobeen; G. Bomba, A. Roufegarinejad, R. Vignos and M. Walters; J. Osteraas; D. Mar; G. Luth; S. Pryor; and R. Serrette. The authors further acknowledge the assistance of several undergraduate research students, C. McEniry and R. McNerney, Professors Conte, Restrepo, and Luco, as well as the support of the staff at NEES@UCSD.

## 8. References

[1] Taylor, A. and Aiken, I, 2012. What's happened to seismic isolation of buildings in the U.S. *Structure Magazine*, March 2012.

[2] Federal Emergency Management Agency (FEMA), 2012. Seismic Performance Assessment of Buildings. Volume 1–Methodology, Tech Rep. FEMA P-58-1, Washington, D.C.

[3] Comerio, M., 1997. Housing issues after disasters. Journal of Contingencies and Crisis Management, **5.3**, 166-178.

[4] Kircher, C.A., Reitherman, R.K., Whitman, R.V., Arnold, C., 1997. Estimation of earthquake losses to buildings. *Earthquake spectra, **13.4***. 703-720.

[5] Ichijo Technological Homes, 2015. Seismic Base Isolation System, available at, http://www.ichijousa.com/page/seismic-base-isolation-system (Last accessed 2015 December 4).

[6] Iiba, M., Midorikawa, M., Yamanouchi, H., Yamaguchi, S., Ohashi, Y., & Takayama, M., 2000. Shaking table tests on performance of isolators for houses subjected to three-dimensional earthquake motions. *Proceedings of the 12th World Conference on Earthquake Engineering*.

[7] Iiba, M., Midorikawa, M., Hamada, H., Yasui, Y., & Hanai, T., 2004. Seismic safety evaluation of base-isolated houses with rubber bearing. *Proceedings of 13th World Conference of Earthquake Engineering*.

[8] van de Lindt, J. W., Liu, H., Symans, M. D., & Shinde, J. K., 2011. Seismic performance and modeling of a half-scale base-isolated wood frame building. *Journal of Earthquake Engineering*, **15.3**, 469-490.

[9] Delfosse, G. C., 1982. Wood framed individual houses on seismic isolators. *Proc. of the International Conf. on Natural Rubber for Earthquake Protection of Buildings and Vibration Isolation*.

[10] Sakamoto, I., Y. Ohashi, and Y. Fujii, 1990. Seismic behavior of base isolated two-storied wooden building. *Proceedings of the 1990 International Timber Engineering Conf.*, Tokyo, Japan.

[11] Reed, J. W., and C. A. Kircher, 1986. Base isolation of a five-story wood-frame building. *Proceedings of a Seminar and Workshop on Base Isolation and Passive Energy Dissipation (ATC-17).*

[12] Symans, Michael D., William F. Cofer, and Kenneth J. Fridley, 2002. Base isolation and supplemental damping systems for seismic protection of wood structures: Literature review. *Earthquake Spectra*, **18.3**, 549-572.

[13] Jampole, E.A., Swensen, S.D., Fell, B., Miranda, E., Deierlein, G.G., 2014, Dynamic Testing of a Low-Cost Sliding Isolation System for Light-Frame Residential Structures. *Proceedings of 10NCEE*, Anchorage, AK.

[14] Swensen, S., 2014. Seismically Enhanced Light-Frame Residential Structures, Ph.D. Thesis, Stanford University, Stanford, CA.

[15] Swensen, S., Acevedo, C., Jampole, E., Miranda, E., Deierlein, G., Hopkins, A., & Fell, B., 2014. Toward damage free residential houses through unibody light-frame construction with seismic isolation, *Proceedings, SEAOC 2014 83rd Annual Convention*, Indian Wells, C.A.

[16] Jampole, E., Deierlein, G., Miranda, E., Fell, B., Swensen, S., and Acevedo, A., 2016. Full scale dynamic testing of a sliding seismically isolated unibody house. *Earthquake Spectra*. Under Review.

[17] Acevedo, A., Deierlein, G., Miranda, E., Fell, B., Swensen, S., and Jampole, E., 2017. Development of a unibody system to improve the seismic performance of lightweight residential wood structures. *Proceedings of 16WCEE*, Santiago, Chile.

[18] Mazzoni, S., McKenna, F., Scott, M.H. and Fenves, G.L., 2006. OpenSees command language manual. *Pacific Earthquake Engineering Research (PEER) Center*.